

The Reddest Quasars II. A gravitationally-lensed FeLoBAL quasar

Mark Lacy^{1,2,3}, Michael Gregg^{2,1}, Robert H. Becker^{2,1}, Richard L. White⁴, Eilat Glikman⁵, David Helfand⁵ and Joshua N. Winn⁶

ABSTRACT

We report the discovery of a $z = 2.65$ low-ionization iron broad absorption line quasar, FIRST J100424.9+122922, which is gravitationally-lensed by a galaxy at $z \approx 0.95$. The object was discovered as part of a program to find very red quasars by matching the FIRST radio survey with the 2-MASS near-infrared survey. J100424.9+122922 is the second lensed system to be found in this program, suggesting that many gravitational lenses are probably missed from conventional optical quasar surveys. We have made a simple lens model and a rough estimate of the reddening in the immediate environment of the quasar which suggests that the quasar is intrinsically very luminous and is accreting at close to the Eddington limit of its $\sim 10^9 M_\odot$ black hole. The lensing galaxy has a small amount of dust which is responsible for some excess reddening observed in the fainter image of the quasar, but is otherwise a fairly typical massive elliptical galaxy. We model the selection effects working against the detection of red quasars in both lensed and unlensed samples. We show that these selection effects are very effective at removing even lightly-reddened high redshift quasars from magnitude-limited samples, whether they are lensed or not. This suggests that the red quasar population in general could be very large, and in particular the class of iron broad absorption line quasars of which J100424.9+122922 is a member may be much larger than their rarity in magnitude-limited samples would suggest.

Subject headings: quasars: individual (J100424.9+122922) – quasars: absorption lines – gravitational lensing – radio continuum: galaxies

¹IGPP, L-413, Lawrence Livermore National Laboratory, Livermore, CA 94550; gregg@igpp.ucllnl.org, bob@igpp.ucllnl.org

²Department of Physics, University of California, 1 Shields Avenue, Davis, CA 95616

³SIRTF Science Center, Caltech, Mail Code 220-6, Pasadena, CA 91125; mlacy@ipac.caltech.edu

⁴Space Telescope Science Institute, Baltimore, MD 21218; rlw@stsci.edu

⁵Columbia University, Department of Astronomy, 550 West 120th Street, New York, NY 10027; eilatg@astro.columbia.edu, djh@astro.columbia.edu

⁶Harvard-Smithsonian Center for Astrophysics, 60 Garden Street, Cambridge, MA 02138; jwinn@cfa.harvard.edu

1. Introduction

We are currently conducting a survey for very red objects selected using the Two-micron All Sky Survey (2MASS; Kleinmann et al. 1994) and the Faint Images of the Radio Sky at Twenty-centimeters survey (FIRST; Becker, White & Helfand 1995; White et al. 1997). We select stellar infrared objects coincident with FIRST radio sources which lack (or have only faint) counterparts on the Palomar Observatory Sky Survey plates. To date we have examined about 100 candidate red quasars, most using Keck or Lick spectroscopy. Of these, ≈ 13 have optical spectra characteristic of $z > 0.5$ quasars reddened by dust (final classification will need to await near-infrared spectroscopy as broad lines sometimes appear in the near-infrared where the extinction to the quasar broad line region is lower). In a previous paper (Gregg et al. 2002) we reported the discovery of two dust-reddened quasars discovered as part of this survey – FIRST J013435.6-093102 and FIRST J073820.1+275045 – one of which (J0134-0931) is gravitationally lensed (see also Winn et al. [2002]). In this paper we describe the recent discovery of a second gravitationally-lensed system, FIRST J100424.9+122922 (hereafter J1004+1229). This quasar is reddened by a combination of dust and extreme, low ionization broad absorption in the rest-frame ultraviolet, making it a member of the rare sub-class of low-ionization broad absorption line quasars, dubbed “FeLoBALs” by Becker et al. (1997), as much of the absorption is due strong absorption from metastable Fe II (Hazard et al. 1987; Becker et al. 1997).

There are two main hypotheses concerning the nature of broad absorption line quasars (BALs). One is that most quasars possess BAL flows, but we only see them if the quasars are viewed at a particular angle to the line of sight which grazes a torus of gas around the nucleus (hereafter the “orientation hypothesis”, e.g. Weymann et al. 1991). The other, which applies particularly for the case of the low-ionisation BALs [LoBALs], is that BALs are quasars at an early stage in their evolution (hereafter the “youth hypothesis”, e.g. Voit, Weymann & Korista 1993). Recently, support for the youth hypothesis has come both from an analysis of the radio properties of BALs in FIRST (Becker et al. 2000), which indicates a range of orientations can produce BAL quasars, and also an apparent association of BALs with infrared-luminous quasars having hosts with merging morphologies and host spectra with “post-starburst” features (Canalizo & Stockton 2001). A further, but more controversial, hint that BALs may represent a stage in the life cycle of a quasar is that BALs may have steep intrinsic X-ray spectral slopes (Mathur et al. 2001; but see also Gallagher et al. 2001 who argue that the X-ray spectral slopes of BALs are not significantly steeper than those of normal quasars). Steep X-ray slopes may be connected with high accretion rates relative to the Eddington limit (Laor et al. 1997), so if BALs do indeed have steeper X-ray slopes this would suggest a link between high accretion rates and the BAL phenomenon. If it is assumed that high accretion rates are typical in the early life of a quasar, perhaps because the supply of fuel capable of falling into the black hole is greatest just after the triggering event, then a consistent picture emerges in which BAL flows are a symptom of high accretion rates produced as radiation pressure from a young quasar close to the Eddington limit pushes away excess material.

The first FeLoBAL to be identified was LBQS 0059-2735 (Hazard et al. 1987). Since then five

more have been found in the FIRST Bright Quasar Survey (FBQS) (Becker et al. 1997; 2000). These objects are overlooked in quasar surveys based on UV/optical color or objective prism selection, not only because of their extreme absorption features and lack of prominent emission lines, but also because, like other LoBALs, they tend to be more heavily reddened by dust than the normal quasar population (Sprayberry & Foltz 1992). Like normal BALs, few are very radio-loud, so they do not appear in surveys with high radio flux density limits either. Quasar surveys based on the FIRST radio survey, are, however, better suited to finding such objects in significant numbers, because of the faint radio flux limit and the lack of the necessity for candidate selection based on exceptionally blue colors.

For our other FIRST/2MASS gravitational lens, J0134-0931, we were unable to determine whether the reddening arose predominately in the immediate environment of the quasar, or in the lensing galaxy. Determining the source of the reddening (and extinction) is critical, however: if heavy reddening by lenses is commonplace, then many gravitationally lensed systems may be missing from optically-based lens surveys. If, on the other hand, the reddening is in the host, then many red quasars may be missing from current quasar surveys, with important implications for attempts to match the mass accreted onto black holes during the “quasar epoch” to the masses of black holes in galaxies today (e.g. Merritt & Ferrarese 2001). An association between BAL quasars and gravitational lensing was noted by Chartas (2000), suggesting that reddening in the hosts usually dominates, but examples of lensed quasars reddened by their lenses are also known [B0218+357 (e.g. Menten & Reid 1996), and PKS 1830-211 (e.g. Wiklind & Combes 1996)].

Our infrared imaging and optical and infrared spectroscopy demonstrate conclusively that J1004+1229 is a lensed FeLoBAL and allow us to derive the basic quantities of the lensing system and also investigate the nature of the lensing galaxy and quasar, as detailed in Sections 2-4. J1004+1229 is the second gravitationally lensed, $z > 0.5$ red quasar found in our survey. This lensing rate (2/13) is much larger than higher that for the overall quasar population, though the statistics are poor so far. In Section 5 we model the effects of lensing and reddening on the optical and near-infrared selection of quasars, attempting to account for this apparently high lensing rate of reddened quasars.

We assume a cosmology with $\Omega_M = 0.3, \Omega_\Lambda = 0.7, H_0 = 60 \text{ km s}^{-1} \text{ Mpc}^{-1}$, unless otherwise stated.

2. Observations

Matching of FIRST and 2MASS showed that the $K' = 14.5$ 2MASS source corresponding to J1004+1229 is 0.3 arcsec from the 12mJy FIRST radio source (compared to estimated rms position errors of 0.2 arcsec in 2-MASS and 0.5 arcsec in FIRST), but that this object was not present on second-generation digitised sky survey plates to a limit of $R \approx 20.8$. In this Section, we describe observations of J1004+1229 in the radio, near-infrared and optical bands. Broad band magnitudes

and radio flux densities for the system are listed in Table 1.

2.1. Spectroscopy

J1004+1229 was initially identified as an FeLoBAL in a Keck ESI spectrum taken on 2000 December 29, though the gravitationally lensed counterimage was not noticed at the time.

Infrared spectroscopy with the NASA Infrared Telescope Facility (IRTF) using NSFCAM was taken on 2001 April 16 (UT) using the K -band grism. The spectrum was nodded up and down the slit in the standard two-point “ABBA” pattern (Eales & Rawlings 1993) to facilitate sky subtraction. A K -band acquisition image showed two components separated by ≈ 1.5 -arcsec which were fortuitously almost aligned with the north-south slit. The spectra show that both components have an emission line at an identical redshift (Figure 1). We denote the bright image as component A, and the faint image as component B throughout this paper.

A further ESI spectrum was taken on 2001 May 26 with the 1-arcsec slit rotated to a sky PA of 9 deg. to include both images of the quasar (Figure 2). Two 900s integrations were taken, and both components of the lensed system were easily resolved along the slit in the $0''.5$ arcsec seeing. The data were calibrated using an observation of Fiege 34.

Figure 3 compares the ESI spectrum of J1004+1229 with two other FeLoBALs, LBQS 0059-2735 (Hazard et al. 1987) and FIRST 1556+3517 (Becker et al. 1997). The similarity of J1004+1229 and FIRST 1556+3517 is evident. Further discussion of the spectrum may be found in Section 3.1. The spectral resolution of the observations is $\approx 2\text{\AA}$, though the spectra have been smoothed to 8\AA resolution in Figures 2 and 3.

2.2. Optical and near-infrared imaging

Infrared images in J and K' were taken with NSFCAM at the IRTF on 2001 April 16. The data were taken in a 9-point mosaic pattern with 60s exposures at each point, and were reduced using the DIMSUM package after flat-fielding with dome flats. The weather was non-photometric and the seeing $0''.7$. V - and I -band images were obtained with the Andalucia Faint Object Spectrograph Camera (ALFOSC) on the Nordic Optical Telescope (NOT) on 2001 April 22 for 3×300 s and 3×600 s respectively, and flat-fielded with twilight flats. Both images show the counterimage component to be extended, most probably due to blending with the lensing galaxy. The images are shown in Figure 4, where we have also attempted to subtract our best estimate of the contribution of the quasar images from the I -band image (see Section 3.2) to reveal the lensing galaxy. Table 1 lists the broad-band magnitudes, flux densities and image-to-counterimage ratios.

2.3. Radio imaging

We observed J1004+1229 at 1.67 GHz with the VLBA⁷ on 8–9 October 2001, using all 10 antennas. We used the compact radio source J1002+1216 as the phase reference (26′ away, peak flux density 0.13 Jy), with a switching time of 5 minutes. The total dwell time on J1004+1229 was 200 minutes.

The data were recorded in eight 8 MHz bands in dual-polarization mode, for a total observing bandwidth of 32 MHz per polarization. Each 8 MHz band was subdivided into 16×0.5 MHz channels. The sampling time was 1 s. For the correlation phase centers, we used the JVAS position (J2000) of the phase reference source ($10^{\text{h}}02^{\text{m}}52^{\text{s}}.8457$, $+12^{\circ}16^{\text{m}}14^{\text{s}}.588$; Browne et al. 1998), and the FIRST position of the target source.

Calibration was performed with standard AIPS tasks. We used a fringe-fitting interval of 2 minutes. Prior to imaging, we averaged the data in time into 6 s bins and in frequency into 1 MHz bins. This level of sampling was sufficient to reduce bandwidth and time-average smearing to less than 1% within $1''.5$ of the phase center. Imaging was also performed with AIPS. We created a $2'' \times 2''$ image centered on the expected A–B midpoint. After component A was subtracted using the CLEAN algorithm, a significant peak ($\sim 9\sigma$) was apparent in the residual image. This peak is the brightest peak in the residual image, it does not belong to the sidelobe pattern of component A, and it is near the expected location of component B. We concluded that it represents component B of the lensed system. The final contour maps, shown in Figure 5, were produced after phase-only self-calibration with a 60 minute solution interval.

When A and B are modeled as elliptical Gaussian components, their flux densities are 6.23 mJy and 0.99 mJy, respectively. The noise on the map is $0.11 \text{ mJy beam}^{-1}$, and the flux density ratio (A/B) is 6.3 ± 0.7 . The overall flux density calibration is uncertain by 5%. Component A is 263.3 ± 1.0 mas west and 1517.2 ± 1.7 mas south of component B. The position of A is (J2000) $10^{\text{h}}04^{\text{m}}24^{\text{s}}.8858$, $+12^{\circ}29^{\text{m}}22^{\text{s}}.313$. The lowest surface-brightness contours of component A suggest the source is partially resolved. The elongation is in a direction nearly perpendicular to the A/B separation, which is suggestive of the tangential stretching that is characteristic of gravitational lensing. However, it is possible that the elongation is an artifact of residual gain errors rather than intrinsic source structure. Further evidence for extended emission comes from the difference between the 1.4 GHz flux density from FIRST of 12.3 mJy, measured in an 5.6-arcsec beam, and the 7.2 mJy total flux measured at 1.67 GHz in the VLBA image. The source has a flux density at 1.4 GHz of 11.8 mJy in the ≈ 45 -arcsec resolution NVSS survey (Condon et al. 1998), identical to the FIRST flux density to within the errors. Thus assuming the difference in flux density between the VLA and VLBA measurements is not due to variability, this suggests the VLBA has resolved out extended emission from the radio source, and also that the source is not significantly larger

⁷The Very Long Baseline Array (VLBA) is operated by the National Radio Astronomy Observatory, a facility of the National Science Foundation operated under cooperative agreement by Associated Universities, Inc.

than the FIRST beamsize.

3. Results and Interpretation

3.1. The quasar spectrum

Our ESI spectra of J1004+1229 show a complicated absorption line spectrum with an apparent edge at 10200\AA , which we ascribe to MgII absorption at $z = 2.65$ (Figures 2 and 3). This interpretation is confirmed by the K -band spectrum, which shows a strong, broad (3500 km s^{-1}) emission line at $2.40\mu\text{m}$, corresponding to $\text{H}\alpha$ at $z = 2.66 \pm 0.01$. Most of the absorption features can be tentatively identified with low-ionization species; for example, MgII 2796/2803 and AlIII 1859 are clearly present. Much of the absorption between these wavelengths is due to metastable excited states of Fe II and perhaps Fe III (Hazard et al. 1987; Becker et al. 1997), hence its classification as an FeLoBAL. The absorbing systems which give rise to the spectral features seem to be quite complex, making the resemblance between J1004+1229 and FIRST 1556+3517 particularly striking (Figure 3). Nevertheless, there are detailed differences in the spectra, for example the Fe I 2167 line, apparently present in FIRST 1556+3517 is absent from J1004+1229. The blueshifts extend to $\approx 10000\text{ km s}^{-1}$ even for the low ionization lines. J1004+1229A has very black absorption troughs, indicating a high covering factor for the absorbing clouds.

3.2. Evidence for lensing

The infrared and optical spectra, which indicate that both components A and B are members of the rare FeLoBAL class of quasar, taken together with the similarity of the image-to-counterimage ratio in the near infrared and the radio indicate that components A and B are almost certainly lensed images of a single quasar. The optical spectra of A and B do, however, differ in detail, and in this section we discuss whether these differences are consistent with lensing.

In a simple, isolated three-image lens system, the brightest component is farthest from the lensing galaxy, and the faintest (demagnified) component is closest. As third images are only rarely detected we modelled the system as containing two images, and assumed that the likely effects of lensing on the spectrum were blending of the weaker component with light from the lensing galaxy, and possibly differential reddening of the two images by dust in the lens. This picture is borne out by the photometry (Table 1): the image-to-counterimage ratio increases from the radio to K' and from K' to J , as one would expect if the counterimage is more strongly reddened, but then decreases again in I as light from the lensing galaxy is blended into that from the counterimage.

We thus attempted to decompose the spectrum of component B into a reddened version of component A plus the lensing galaxy. Fortunately the large number of strong features in the spectrum of the quasar makes this relatively easy to do. The unknown nature and redshift of the

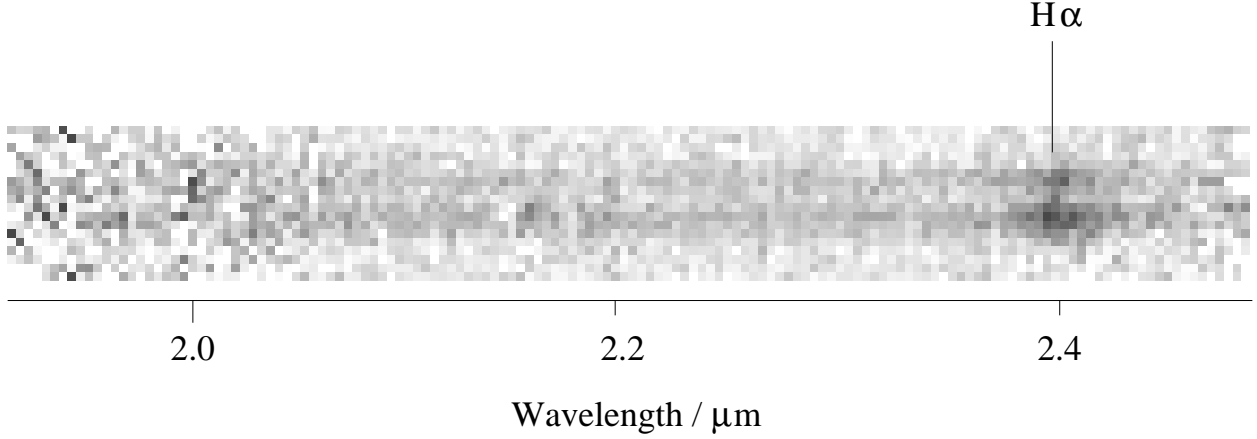


Fig. 1.— K -band spectrum of J1004+1229, obtained with NSFCAM at the IRTF, showing the H α emission line in the two components A (lower) and B (upper).

Band	Mag/Flux	A/B ratio
V	22.9 ± 0.1	~ 4
I	19.7 ± 0.1	4.1 ± 0.5
J	16.55 ± 0.16	7.7 ± 0.2
K'	14.54 ± 0.09	6.8 ± 0.2
1.4 GHz	12.3 mJy	-
1.67GHz	-	6.3 ± 0.7

Table 1: Photometry and image ratios for the J1004+1229 system. Near-IR photometry is from the 2-MASS catalogue, optical photometry from our NOT observations and the radio flux density from FIRST. Image-to-counterimage ratios were determined from PSF fitting using DAOPHOT on our NOT and IRTF data in I , J and K' . The signal-to-noise ratio in the V -band image was too low to permit a reliable measurement of the A/B flux ratio.

Quasar redshift	2.65 ± 0.01
Quasar M_B	$-28.5 + 2.5\lg(\mu/3) - 2.5\lg(f_B/3)$
1.4GHz radio luminosity	$2 \times 10^{25} \times (3/\mu)\text{WHZ}^{-1}\text{sr}^{-1}$
Lens redshift	0.95 ± 0.01
Lens M_B	≈ -21.1
Lens σ_v	$\approx 240\text{kms}^{-1}$
Lens M/L_B	$\approx 11hM_\odot/L_\odot$

Table 2: Derived quantities for the J1004+1229 system. The lensing magnification of the quasar is denoted μ , and dust attenuation factor in rest-frame B -band f_B . The radio flux is assumed to originate entirely from the quasar. The mass-to-light ratio is quoted for $H_0 = 100h\text{kms}^{-1}\text{Mpc}^{-1}$

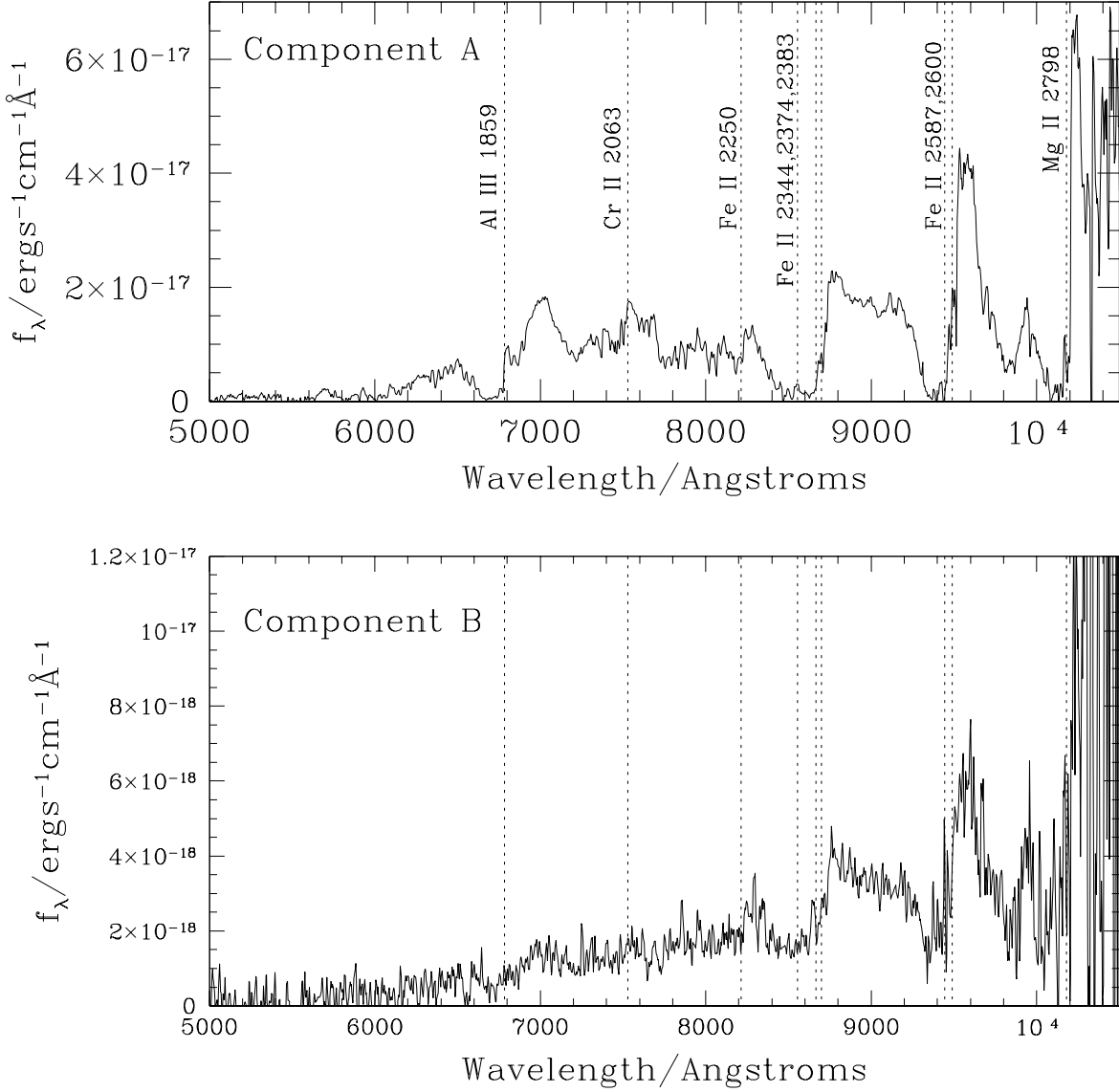


Fig. 2.— The spectrum of components A and B of J1004+1229. The spectral resolution in these smoothed spectra is 8\AA . The dotted lines, labelled in the upper panel, mark the redshifted wavelengths of some of the stronger broad absorption features in the spectrum.

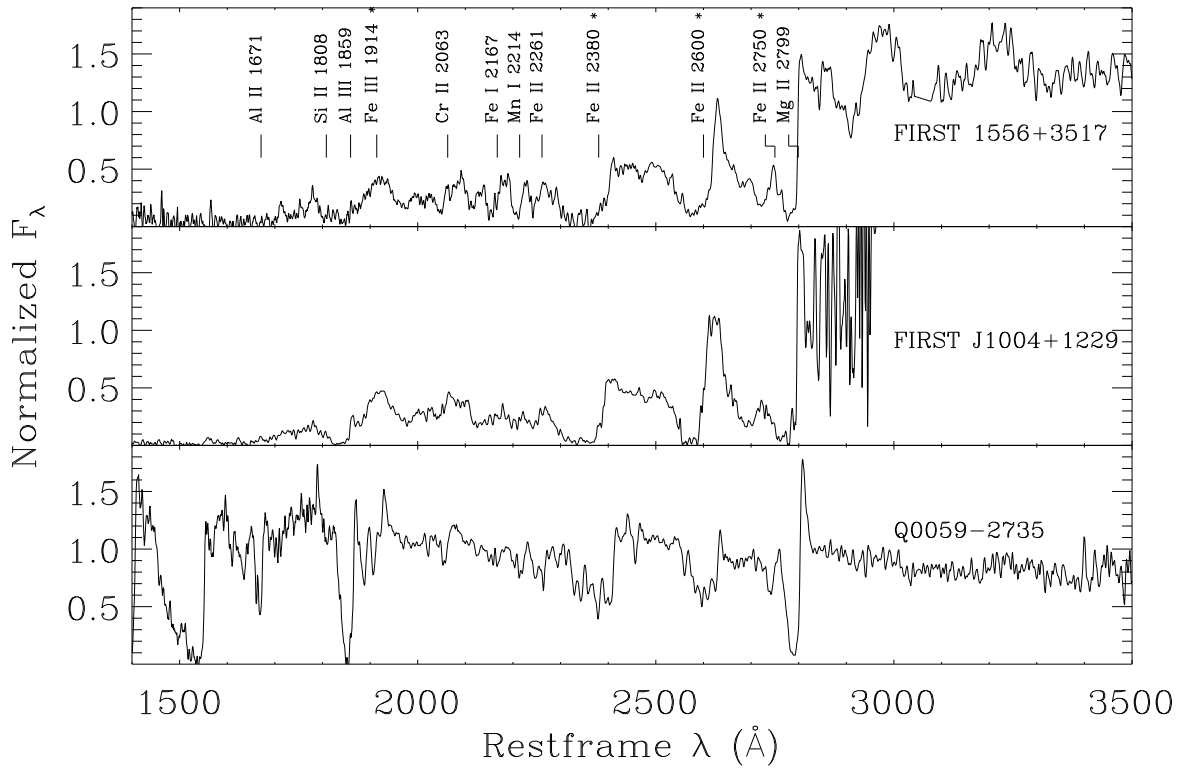


Fig. 3.— The spectrum of J1004+1229A compared to that of the FIRST FeLoBAL J1556+3517 and the original FeLoBAL, Q0059-2735 (Hazard et al. 1987). The similarity of J1004+1229 to J1556+3517 is particularly strong. Prominent absorption features typically found in FeLoBALs are marked; the asterisk denotes a metastable state.

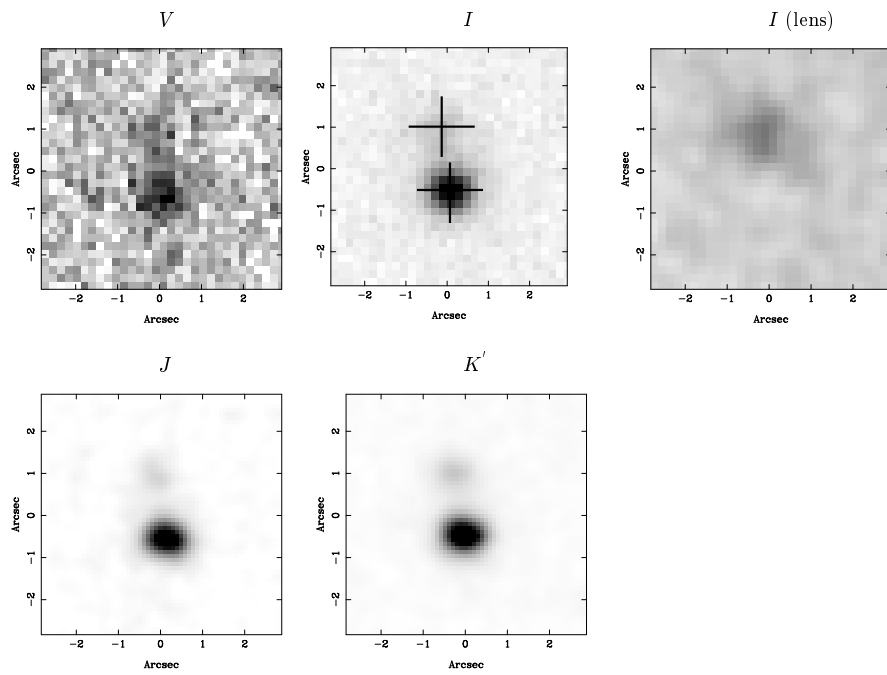


Fig. 4.— Images of J1004+1229. Top row, left to right: *V*, *I*, and the *I*-band image with our best estimate of the the two lensed quasar images subtracted to reveal the lensing galaxy. Bottom row, left to right: *J* and *K'*. Crosses on the *I*-band image mark the positions of the radio components detected with the VLBA (see Figure 5).

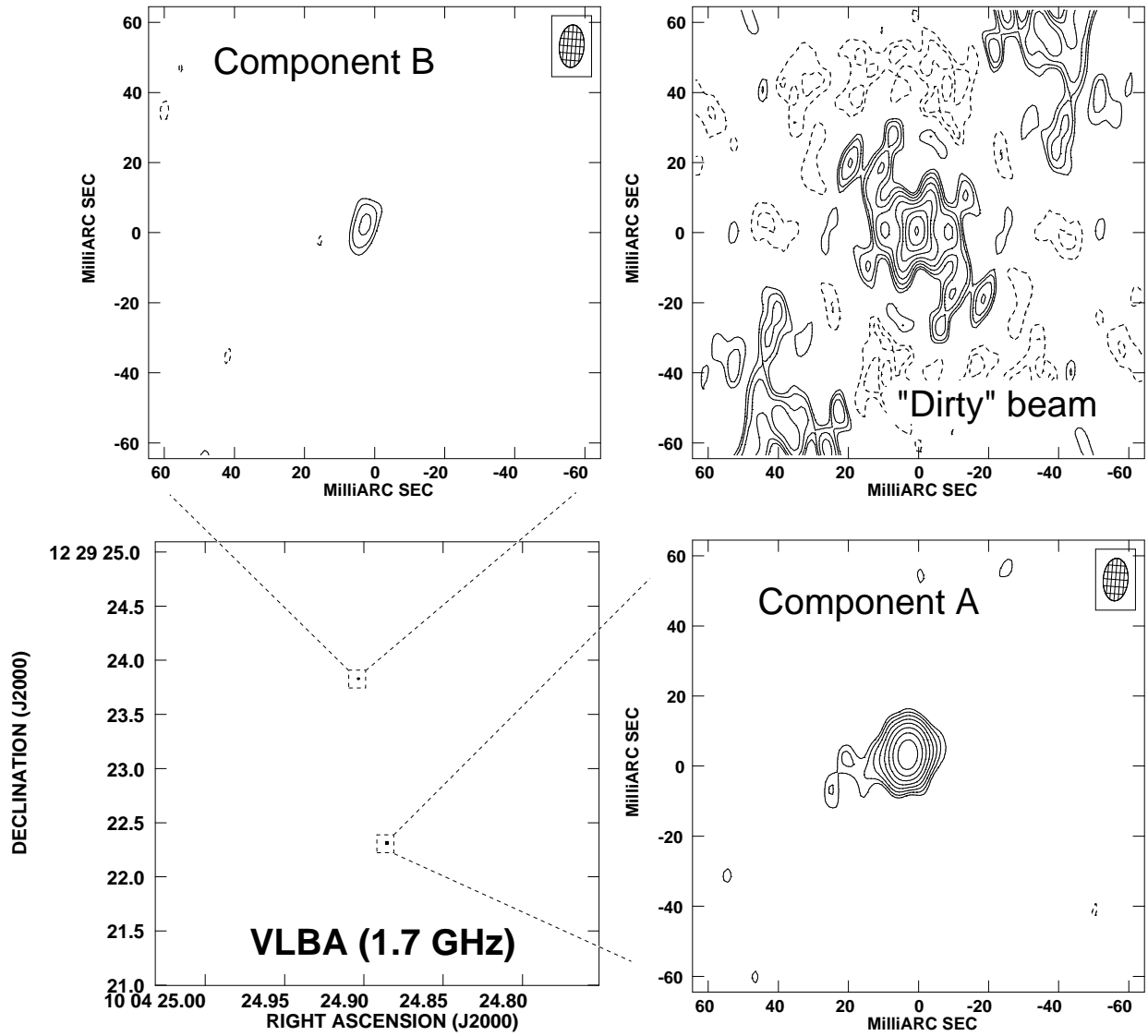


Fig. 5.— The 1.7 GHz VLBA image of J1004+1229. The bottom left panel shows the whole map, with the bottom right and top left panels showing close-ups of components A and B respectively. The dirty beam is shown in the top-right panel.

lensing galaxy mean that a large parameter space would need to be covered in a full analysis; we have therefore decided to restrict ourselves to a fairly coarse grid of reddenings to simplify the problem.

We explored reddening values of $E(B - V)$ from 0 to 0.5 in steps of 0.1, assuming a ratio of selective to total extinction, $R_V = 3.1$ and a Milky Way extinction law (Cardelli, Clayton & Mathis 1989) (Figure 6). Initially we assumed a lens redshift $z_L = 1$ at which we applied the extinction. We fixed the true image:counterimage ratio by estimating the excess reddening of component B at K -band and then divided the K -band image:counterimage ratio by this excess reddening factor.

An $E(B - V) \approx 0.2$ was found to best remove the quasar features from the spectrum of B, leaving a residual which is smooth apart from a break at 7800\AA . We interpret this as a 4000\AA break at $z = 0.95$. In the lower panel of Fig. 6 we show the residuals from subtracting normalized, reddened spectra of component A from that of component B for reddenings of $E(B - V) = 0.1, 0.2$ and 0.3 at the lens redshift. The intrinsic flux ratio we obtain for the best-fit, namely 5.5 is a little lower than the 6.3 obtained from the VLBA data (though only by 1.2σ). Inspection of Figure 6 seems to indicate that the intrinsic flux ratio lies between 5 and 6.2 (corresponding to reddening by the lens between $E(B - V) = 0.1$ and 0.3), but spatially-resolved spectroscopy of the lens is required to make a more accurate estimate.

As the resolution of our images is insufficient to show the lens resolved from component B, we adopted a simple singular isothermal sphere model with which to extract the rough physical parameters of the lens system. In this model, the image to counterimage ratio is given by:

$$R = \frac{\alpha + \theta_s}{\alpha - \theta_s},$$

where θ_s is the angle between the source position and the lens center, and α is the deflection angle induced by the lens (which for this model is independent of impact parameter). The bright and faint images are offset by $\alpha + \theta_s$ and $\alpha - \theta_s$ from the lens center, respectively. Thus given the image:counterimage ratio of 5.5 and separation (2α) of 1.54 arcsec, we expect the fainter image to be offset by 0.24 arcsec from the lens, consistent with us failing to resolve them in our images. The total magnification in this model is $2\alpha/\theta_s = 2.9$.

We derive a velocity dispersion for the lens of $\approx 240\text{km s}^{-1}$, a mass within the Einstein radius of $\approx 3.0 \times 10^{11} M_\odot$, and a blue mass-to-light ratio of $\approx 11h$ in solar units (where $H_0 = 100h\text{km s}^{-1}\text{Mpc}^{-1}$), all of which are consistent with the lens being a massive elliptical galaxy. The optical magnitude estimated from the spectra and the I -band image is also consistent with this, and suggests that the galaxy has a stellar luminosity about 0.5 magnitudes brighter than M_B^* at zero redshift.

4. Discussion

4.1. The dust in the lensing galaxy

The low but non-zero value for the excess reddening produced by the lensing galaxy is at the upper end of the range observed for local ellipticals (e.g. Goudfrooij & de Jong 1995), and also those inferred for other quasars lensed by $0.3 \lesssim z \lesssim 1$ elliptical galaxies (Falco et al. 1999). Elliptical galaxies at $z \sim 1$, however, are more likely to have low-level star formation episodes occurring in their cores (Menanteau, Abraham & Ellis 2001), so it is possible that such galaxies would typically have more dust in their inner few kpc than is usually seen either in local ellipticals or in $z \sim 0.5$ lensing galaxies.

4.2. The intrinsic nature of the quasar

LoBALs are in general redder than normal quasars, almost certainly because of reddening in the quasar environment. Estimating the reddening of this quasar is difficult because of the strong absorption features in the rest-frame UV. If, however, J1004+1229 is like lower redshift FeLoBALs there should be little line absorption longward of MgII 2798, and we can make a very rough estimate of the reddening by comparing the observed optical to near-infrared spectral energy distribution (SED) with that expected from a normal FBQS quasar at this redshift. We assume that the effect of reddening in the lens is negligible compared to that in the quasar environment: we expect dust only in the inner few kpc of the elliptical, and, as discussed above, this has only a small effect on the fainter image; the brighter image, with an impact parameter ~ 10 kpc is unlikely to be significantly reddened by dust in the lens. In Figure 7 we plot a comparison of the SED of J1004+1229 with that of FBQS composites (Brotherton et al. 2001) reddened with the Small Magellanic Cloud (SMC) extinction law of Pei (1992), from which we estimate an $A_V \sim 1$ mag. This is similar to the $A_V \sim 1.5$ estimated for the FeLoBAL J1556+3517 by Najita, Dey & Brotherton (2001) (see also Fig. 1).

With a radio luminosity at 5GHz, $L_{5\text{GHz}} \sim 10^{25} \text{WHz}^{-1} \text{sr}^{-1}$ after correction for lensing, the quasar is in the radio-intermediate class when this is defined through radio luminosity. In terms of the radio-to-UV continuum ratio R^* (Sramek & Weedman 1980), $R^* \approx 280$ before correction of the UV flux for reddening and BAL absorption. After correction by an assumed $E(B - V) = 0.35$ for reddening, and an estimated BAL absorption of a further factor of two, this results in an $R^* \approx 10$, again placing the quasar in the radio-intermediate class, as is typical for BALs in FIRST (Becker et al. 2000; 2001).

At restframe optical wavelengths the extinction due to dust approximately matches the magnification due to gravitational lensing, and using this assumption we can use the width of the H α line to estimate a black hole mass of a few times $10^9 M_\odot$, following the prescription used by Lacy et al. (2001). Even with this high black hole mass, the high intrinsic luminosity of the quasar requires

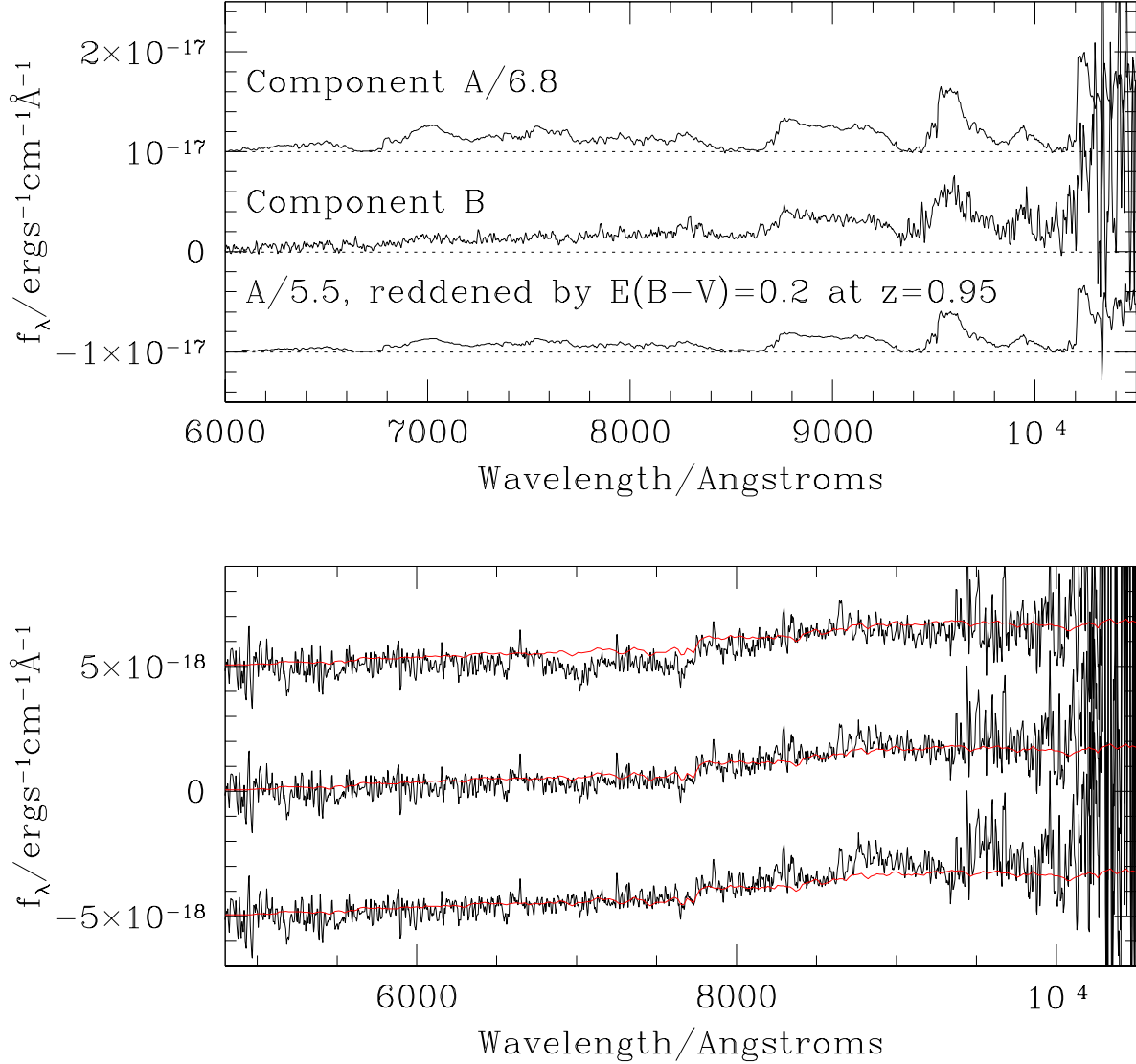


Fig. 6.— Decomposition of the Keck ESI spectrum. Top panel: raw spectrum of component B (middle spectrum) compared to the spectrum of A divided by the K -band flux ratio of 6.8 (upper spectrum) and the spectrum of A reddened by $E(B - V) = 0.2$ at $z = 0.95$, divided by 5.5 (lower spectrum). Lower panel: residuals obtained by subtracting from the spectrum of component B spectra of component A reddened in the rest-frame of the lens and normalized to the K -band flux ratio. From top to bottom: A reddened by $E(B - V) = 0.1$ and divided by 6.2; A reddened by $E(B - V) = 0.2$ and divided by 5.5, and A reddened by $E(B - V) = 0.3$ and divided by 5. Superposed in red on all three spectra is a 6Gyr old, 1Gyr burst galaxy model from the PEGASE library of Fioc & Rocca-Volmerange (1997) redshifted to $z = 0.95$, our best estimate of the lens redshift.

that it is accreting near the Eddington limit. The high black hole mass is consistent with its high radio luminosity for a BAL quasar.

5. Lensing of red quasars

The steep number counts of high luminosity quasars produces a large magnification bias, i.e. a tendency for lensed quasars to be over-represented in a flux-limited quasar survey (e.g. Turner, Ostriker & Gott 1984). This typically results in such samples containing $\sim 1\%$ of lensed quasars, compared to $\sim 0.1\%$ expected in the absence of magnification bias. As our 2MASS quasar sample is very bright, the magnification bias is even higher than usual, and, using the lensing model discussed below, we estimate that the expected lensing rate for $z > 0.5$ quasars in our sample is $\approx 3\%$. Even so, the discovery that 2/13 of our $z > 0.5$ luminous red quasars are lensed is surprising. Although the numbers of quasars and lenses in our sample is small, the Poisson probability of finding two or more lensed quasars in our sample by chance is only 0.06. Why the lensed fraction is so high is not clear, but it is probably linked to the observation of Chartas (2000) who showed that the fraction of lensed quasars which are BALs is higher than that in normal quasar samples. Chartas argues that the fraction of attenuated BAL quasars in samples of gravitationally-lensed quasars can be explained as a result of the joint effects of lensing and attenuation on the selection of these samples. His analysis is strongly dependent on the relative amounts of attenuation by dust and magnification by lensing, in addition to the slope of the luminosity function. To see this, we follow Goodrich (1997) and Chartas (2000) by considering a quasar population with a luminosity function $\phi(L, z)$ studied in a narrow range of luminosity (L_1, L_2) at redshift z . We draw samples of lensed quasars magnified by a mean magnification factor M , and reddened quasars (including BALs), attenuated by a mean attenuation factor A . We also now define the probability of the quasar being lensed by p_l , and the probability of it being significantly reddened by p_r . The fraction of lensed quasars in the sample is f_l :

$$f_l = \frac{\Phi(L_1/M, L_2/M, z)}{\Phi(L_1, L_2, z)} p_l = b_l p_l$$

where Φ is the integral luminosity function and b_l is the usual lensing magnification bias factor (e.g. Turner, Ostriker & Gott 1984). The fraction of red quasars in the sample is f_r :

$$f_r = \frac{\Phi(L_1 A, L_2 A, z)}{\Phi(L_1, L_2, z)} p_r = b_r p_r$$

where we define b_r as the “attenuation bias factor”, by analogy with b_l . If the luminosity function is steep (i.e., equivalent to a power-law of index < -1 over the luminosity ranges of interest), then $b_l > 1$ and $b_r < 1$. The fraction of lensed quasars which are reddened, f_{lr} is then:

$$f_{lr} = \frac{\Phi(L_1 A/M, L_2 A/M, z)}{\Phi(L_1/M, L_2/M, z)} p_r.$$

Hence if $A \approx M$ and the luminosity function is a single power-law, then $f_{lr} = p_r/b_l \approx b_r p_r = f_r$, i.e. the same as in the rest of the sample. It is, however, suggestive in this context that both the lensed

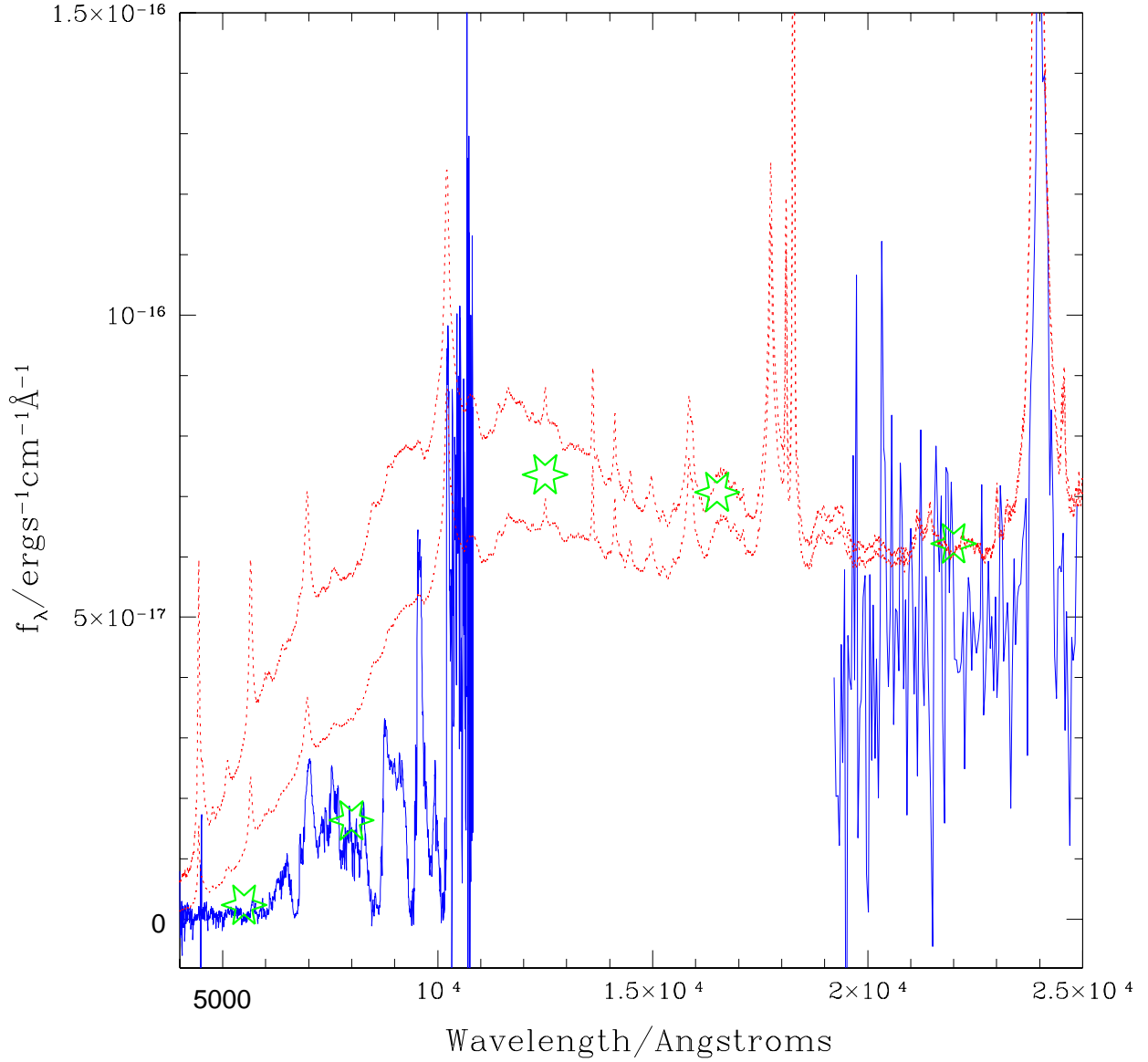


Fig. 7.— The spectrum of J1004+1229A (solid blue line) compared to the FBQS composite spectrum (Brotherton et al. 2001) reddened by $E(B - V) = 0.3$ and $E(B - V) = 0.4$ (upper and lower red dotted lines respectively). Points from the 2-MASS J, H, K and our NOT V and I -band photometry of the system are shown as green stars. The optical and infrared spectra have been scaled to match the broad-band magnitudes in I and K respectively.

objects are amongst the brightest in K -band of all our FIRST-2MASS quasar candidates, where b_l should be highest. A steep cutoff in the luminosity function at high luminosities could have the effect of dramatically decreasing b_r (as there are very few high luminosity quasars to attenuate) whilst keeping b_l moderate. No evidence for such a cutoff has been found, however (e.g. Wisotzki 2000).

We now make the discussion more quantitative, by considering hypothetical quasar surveys selected in the K -band, with magnitude limits of $K = 15$, typical of the deeper portions of 2MASS, and $K = 18$, which would be typical of future large-area near-infrared surveys with 4-m class telescopes, and B -band selected samples at $B = 18$ and $B = 21$. We adopt the luminosity function of Boyle et al. (2000)⁸, and assume an optical spectrum whose flux density $f_\nu \propto \nu^{-0.5}$. We take the lensing probability $p_l(z)$ from Kochanek (1993), and integrate over the magnification distributions of King & Browne (1996). The distribution of attenuations in the quasar population is uncertain. The only sample for which this has been well-studied is the extremely radio-bright 3C sample, which, of course, may well not be typical of the quasar population as a whole, and contains no BALs. Simpson, Rawlings & Lacy (1999) find that, in a total sample of ≈ 32 $z \sim 1$ 3C radio sources, $28^{+25}_{-13}\%$ of quasars are significantly reddened with A_V values ranging from ≈ 2 to ≈ 15 . Given the difficulty of defining a plausible attenuation distribution we have decided to investigate how the fraction of reddened quasars in both lensed and unlensed samples varies as a function of attenuation, using the SMC extinction law of Pei (1992). In Fig. 8, we plot the fraction of reddened quasars expected in magnitude limited samples as a function of attenuation in the rest-frame at $z = 2$ in both lensed and unlensed samples, selected in K -band and B -band. The plots are normalized to unity for zero attenuation. Even for samples selected in the near-infrared, red quasars with rest-frame $A_V \gtrsim 1$ are strongly selected against. This is particularly true in bright samples, where the slope of the luminosity function is steepest. Also, although the fraction of red quasars in lensed samples is higher than that in unlensed samples, it remains a factor of several lower than the true fraction. These numbers depend only on the magnitude limit of the quasar sample and the band to which that limit is applied, and are independent of other selection criteria which might further decrease the number of red quasars in a sample, e.g. a blue color selection criterion. Our model implies that the high fraction of red quasars seen in lensed samples is not likely to be entirely due to magnification bias effects, if the assumption that reddened and unreddened quasars are drawn at random from the same underlying population is correct. In the B -band, where quasar samples are typically selected, the selection effects are even more pronounced, and in a $B \approx 18$ magnitude-limited sample (e.g. LBQS) very few $z > 2$ quasars reddened by $A_V > 1$ in the rest-frame would ever be found.

⁸At $z \sim 2$ this luminosity function is consistent with that of Wisotzki (2000), which, although it is only applicable to the bright end, covers the range of magnitudes which includes our very luminous quasars.

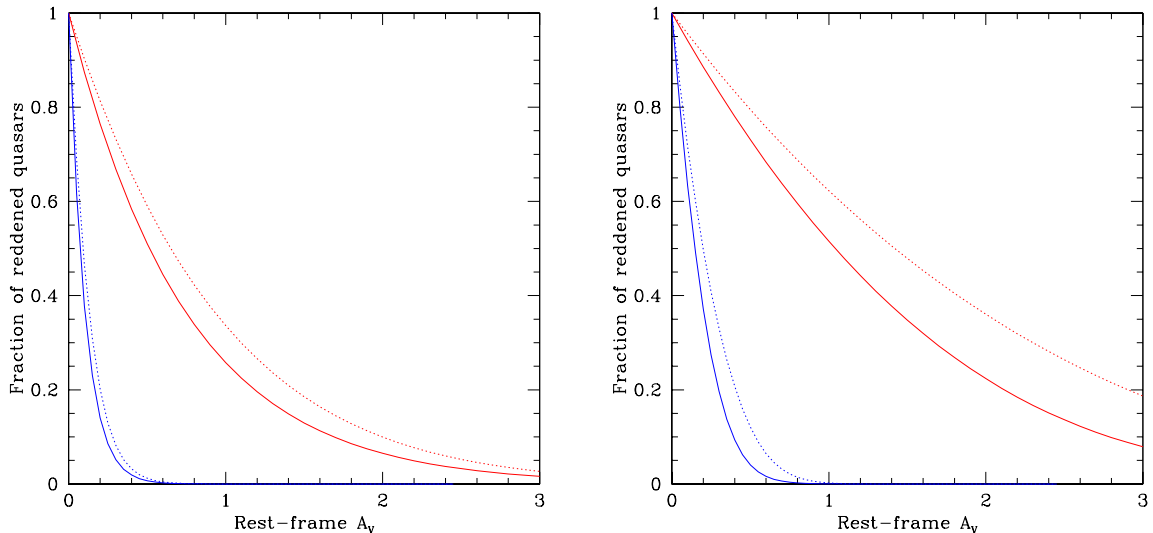


Fig. 8.— The fraction of red quasars in magnitude-limited samples at $z = 2$ as a function of rest-frame extinction. Left: the solid and dotted curves correspond to normal and lensed quasar samples in $K = 15$ (red) and $B = 18$ (blue) samples. Right: the same for a sample with a $K = 18$ (red) and a $B = 21$ (blue) magnitude limit. For comparison, J1004+1229 has $A_V \approx 1$ and J0134-0931 (lensed) and J0738+2927 (not lensed; Gregg et al. 2001) have $A_V \approx 2$.

An alternative explanation for the high fraction of red lensed quasars is that red quasars are a distinct population, as might be the case if redness is a phase in a quasar’s life cycle rather than a purely geometrical effect. This is consistent with the interpretation of BAL QSOs, especially the FeLoBALs, as being an early or heavily obscured phase in the lives of quasars (Voit et al. 1993; Egami et al. 1996; Becker et al. 1997, 2000; Gregg et al. 2000). If the luminosity function for red quasars is significantly steeper than for normal quasars, then this could lead to a higher than normal magnification bias in samples of red quasars, and explain our seemingly large lensing rate, as well as the tendency for the fraction of BAL QSOs in lensed samples to be higher. A physical basis for this might be that the luminosity function of quasars accreting at close to the Eddington rate will resemble the black hole mass function, which has a steep slope at high masses caused by the cutoff in galaxy masses produced by the Schechter function (e.g. Salucci et al. 1999). The only way for a geometrical model to be consistent with this result is if the range of angles over which the quasar is seen as significantly reddened increases as quasar luminosity decreases.

6. Conclusions

The comparison of FIRST and 2MASS has allowed us to discover quasars reddened by dust, both intrinsic and intervening. J1004+1229 is almost entirely reddened in the local environment of the quasar by a combination of dust and strong low ionization absorption features; the lens

contributing only a small amount of reddening, and probably only to the fainter lensed image.

Even after taking into account magnification by lensing, the quasar is intrinsically very luminous and contains a supermassive black hole, probably accreting at close to the Eddington rate. The apparently high frequency of lensing among our red quasars could be explained in a model in which red quasars have an intrinsically steeper luminosity function than the normal quasar population, although if the geometry of the reddening material is such that the range of angles in which reddening is seen increases as quasar luminosity decreases, a geometrical explanation could also work. In either case, the extent to which high-redshift, dust-reddened quasars in both lensed and unlensed are selected against in bright quasar surveys is very great, and suggests that a large fraction of quasars are missed from surveys with optical or near-infrared selection. In particular it suggests that FeLoBALs, selected against both because of dust reddening and extreme rest-frame UV absorption, may be much more common than their rarity in magnitude-limited samples would suggest. When we complete our FIRST/2MASS survey, and analyse the results in the context of our modelling we should obtain a good estimate of the true fraction of red quasars in quasar samples of much more moderate radio luminosity than those in the 3C survey.

The lensed nature of J1004+1229 gives us a unique opportunity to study the host galaxy of a high-redshift BAL through deep imaging with NICMOS on HST, or with ground-based adaptive optics. If red quasars and BALs are indeed a distinct and early phase in quasar evolution, study of the host galaxy of J1004+1229 may help reveal the phenomena responsible for creating such objects.

We thank Per Lilje for taking the *V*- and *I*-band images of J1004+1229 on the NOT, and Mike Brotherton for helpful discussions. ML was a visiting Astronomer at the Infrared Telescope Facility, which is operated by the University of Hawaii under contract from the National Aeronautics and Space Administration. The NOT is operated on the island of La Palma jointly by Denmark, Finland, Iceland, Norway, and Sweden, in the Spanish Observatorio del Roque de los Muchachos of the Instituto de Astrofísica de Canarias. ALFOSC is owned by the Instituto de Astrofísica de Andalucía (IAA) and operated at the NOT under agreement between IAA and the NBIfAFG of the Astronomical Observatory of Copenhagen. The Two Micron All Sky Survey (2MASS) is a joint project of the University of Massachusetts and the Infrared Processing and Analysis Center/California Institute of Technology, funded by the National Aeronautics and Space Administration (NASA) and the National Science Foundation (NSF). This work was mostly performed under the auspices of the U.S. Department of Energy, National Nuclear Security Administration by the University of California, Lawrence Livermore National Laboratory under contract No. W-7405-Eng-48, with additional support from NSF grants AST-98-02791 (University of California, Davis) and AST-98-02732 (Columbia University), with some work carried out at the Jet Propulsion Laboratory, California Institute of Technology, under contract with NASA.

REFERENCES

- Becker, R.H., White, R.L., Helfand, D.J. 1995, *ApJ*, 450, 559
- Becker R.H., Gregg M.D., Hook I.M., McMahon R.G., White R.L., Helfand D.J., 1997, *ApJ*, 479, L93
- Becker R.H., White R.L., Gregg M.D., Brotherton M.S., Laurent-Muehleisen S.A., Arav N., 2000, *ApJ*, 538, 72
- Becker R.H., et al., 2001, *ApJS*, 135, 227
- Boyle B.J., Shanks T., Croom S.M., Smith R.J., Miller L., Loaring N., Heymans C., 2000, *MNRAS*, 317, 1014
- Brotherton M.S., Tran H.D., Becker R.H., Gregg M.D., Laurent-Muehleisen S.A., White R.L., 2001, *ApJ*, 546, 775
- Browne I.W.A., et al., 1998, *MNRAS*, 293, 257
- Canalizo G., Stockton A.N., 2001, in, Crenshaw D.M., Kraemer S.B., George I.M., eds, *Mass Outflows in Active Galactic Nuclei: New Perspectives*. ASP Conf. Ser. in press (astro-ph/0107323)
- Cardelli J.A., Clayton G.C., Mathis J.S., 1989, *ApJ*, 345, 245
- Chartas G., 2000, *ApJ*, 531, 81
- Condon, J.J., Cotton W.D., Greisen E.W., Yin Q.F., Perley R.A., Taylor G.B., Broderick J.J., 1998, *AJ*, 115, 1693
- Cowie L.L., et al., 1994, *ApJ*, 432, L83
- Eales S.A., Rawlings S., 1993, *ApJ*, 411, 67
- Egami, E., Iwamuro, F., Maihara, T., Oya, S., & Cowie, L. L. 1996, *AJ*, 112, 73
- Falco E., Impey C.D., Kochanek C.S., Lehár J., McLeod B.A., Rix H.-W., Keeton C.R., Muñoz J.A., Peng C.Y., 1999, *ApJ*, 523, 617
- Fioc M., Rocca-Volmerange B., 1997, *A&A*, 326, 950
- Gallagher, S.C., Brandt W.N., Chartas G., Garmire, G., 2001, *ApJ*, in press (astro-ph/0110579)
- Goodrich R.W., 1997, *ApJ*, 474, 606
- Goudfrooij P., de Jong T., 1995, *A&A*, 298, 784

- Gregg, M. D., Becker, R. H., Brotherton, M. S., Laurent-Muehleisen, S. A., Lacy, M., & White, R. L. 2000. *ApJ*, 544, 142
- Gregg M.D., Lacy M., White R.L., Glikman E., Helfand D., Becker R.H., Brotherton M.S., 2001, *ApJ*, 564, 133
- Hazard C., McMahon R.G., Webb J.K., Morton D.C., 1987, *ApJ*, 323, 263
- Kleinmann, S.G., Lysaght, M.G., Pughe, W.L., Schneider, S.E., Skrutskie, M.F., Weinberg, M.D., Price, S.D., Matthews, K., Soifer, B.T., Huchra, J.P. 1994, *ApJS*, 217, 11
- King L.J., Browne I.W.A., 1996, *MNRAS*, 282, 67
- Kochanek C.S., 1993, *MNRAS*, 261, 453
- Lacy M., Laurent-Muehleisen S.A., Ridgway S.E., Becker R.H., White R.L., 2001, *ApJ*, 551, L17
- Laor A., Fiore F., Elvis M., Wilkes B.J., McDowell J.C., 1997, *ApJ*, 477, 93
- Mathur S., Matt G., Green P.J., Elvis M., Singh K.P., 2001, *ApJ*, 551, L13
- Menanteau F., Abraham R.G., Ellis R.S., 2001, *MNRAS*, 322, 1
- Menten K.M., Reid M.J., 1996, *ApJ*, 465, L99
- Merritt D., Ferrarese L., 2001, *MNRAS*, 320, L30
- Najita J., Dey A., Brotherton M.S., 2000, *AJ*, 120, 2859
- Pei Y.C., 1992, *ApJ*, 395, 130
- Salucci P., Szuszkiewicz E., Monaco P., Danese L., 1999, *MNRAS*, 307, 637; erratum *MNRAS* 311, 448
- Simpson C., Rawlings S., Lacy M., *MNRAS*, 306, 828
- Sprayberry D., Foltz C.B., 1992, *ApJ*, 390, 39
- Sramek R.A., Weedman D.W., 1980, *ApJ*, 238, 435
- Turner E.L., Ostriker J.P., Gott J.R., 1989, *ApJ*, 284, 1
- Voit G.M., Weymann R.J., Korista K.T., 1993, *ApJ*, 413, 95
- Weymann R.J., Morris S.L., Foltz C.B., Hewett P.C., 1991, *ApJ*, 373, 23
- White, R.L., Becker, R.H., Helfand, D.J., Gregg, M.D. 1997, *ApJ*, 475, 479
- Wiklind & Coombes, 1996, *Nat*, 379, 139

Winn J.N., Lovell J.E.J., Chen H.-W., Fletcher A.B., Hewitt J.N., Patnaik A.R., Schechter P.L.,
2001, ApJ, 564, 143

Wisotzki L., A&A, 353, 853